Nonlinear Adaptive Excitation Control for Structure Preserving Power Systems

Yong Wan, and Federico Milano, *Fellow, IEEE*

***Abstract*—The paper proposes a decentralized excitation controller to improve the stability of large power systems. Extended Lyapunov-like energy function and equivalent expressions of stator transient voltages are utilized to design a nonlinear adaptive excitation controller. The proposed controller only requires local machine measures and parameters. The performance of the designed excitation control system is evaluated on the well-known IEEE 118-bus 54-unit power system and compared with conventional exciter controls.**

***Index Terms*—Multi-machine power systems, automatic voltage control, structure preserving model, transient stability analysis, decentralized control, Lyapunov function.**

NOMENCLATURE

SPM	Structure preserving model.
RNM	Reduced-network model.
AEC	Adaptive excitation controller.
RNC	RNM-based excitation controller.
m	Number of machines.
b	Number of buses.
$l, k, (j)$	Index of (machine) bus.
Ω_l	Index set of buses which connect to bus l.
Ω	Index set of branches, $k \in \Omega_l \Rightarrow lk \in \Omega$.
$\bar{b}, (\bar{m})$	Index set of (machine) buses, $\bar{m} \subseteq \bar{b}$.
Z_0	Equilibrium value of any variable Z.
$\dot{Z}$	Time derivative of any variable Z.
$\mathrm{Hess}(\cdot)$	Hessian matrix of a function.
V_{t_l}	Voltage magnitude of bus l, in pu.
$\boldsymbol{V}$	Voltage magnitude vector.
θ_l	Voltage angle of bus l, in rad.
$\boldsymbol{\theta}$	Voltage angle vector.
δ_j	Power angle of jth machine, in rad.
$\boldsymbol{\delta}$	Power angle vector.
$\tilde{\delta}_j, \theta_{lk}$	Relative angles $\tilde{\delta}_j = \delta_j - \theta_j$, $\theta_{lk} = \theta_l - \theta_k$.
V_{d_j}, V_{q_j}	$V_{d_j} = -V_{t_j} \sin \tilde{\delta}_j$, $V_{q_j} = V_{t_j} \cos \tilde{\delta}_j$.
$\tilde{V}_{sj}, \tilde{V}_{cj}$	$\tilde{V}_{sj} = V_{d_{j0}} - V_{d_j}$, $\tilde{V}_{cj} = V_{q_j} - V_{q_{j0}}$.
ω_j	Relative speed of jth machine, in rad/s.
$\boldsymbol{\omega}$	Relative speed vector.
f_0	System frequency.
ω_s	Synchronous speed $\omega_s = 2\pi f_0$, in rad/s.
S_{ω_j}	Relative speed $S_{\omega_j} = \omega_j/\omega_s$, in pu.
E'_{d_j}, E'_{q_j}	d- and q-axis stator transient voltages of jth machine, in pu.
$\tilde{E}_{dj}, \tilde{E}_{qj}$	$\tilde{E}_{dj} = E'_{d_j} - E'_{d_{j0}}$, $\tilde{E}_{qj} = E'_{q_j} - E'_{q_{j0}}$.
$\boldsymbol{E'_d}, \boldsymbol{E'_q}$	d- and q-axis stator transient voltages vector.
E_{fd_j}	Excitation voltage of jth machine, in pu.
$\boldsymbol{x}$	Vector $\left[\boldsymbol{V}^{\mathrm{T}}\ \boldsymbol{\theta}^{\mathrm{T}}\ \boldsymbol{\delta}^{\mathrm{T}}\ \boldsymbol{\omega}^{\mathrm{T}}\ \boldsymbol{E'_d}^{\mathrm{T}}\ \boldsymbol{E'_q}^{\mathrm{T}}\right]^{\mathrm{T}}$.
H_j	Inertia constant of jth machine, in s.
D_j	Damping coefficient of jth machine, in pu.
P_{m_j}	Mechanical power of jth machine, in pu.
P_{e_j}, Q_{e_j}	Active and reactive powers generated by jth machine, in pu.
$\boldsymbol{P_e}$	Active power vector.
P_{lk}, Q_{lk}	Active and reactive powers transmitted on the line between bus l and bus k, in pu.
P_{L_l}, Q_{L_l}	Active and reactive powers consumed by the load at bus l, in pu.
G_{lk}	Conductance of the line between bus l and bus k, in pu.
$B_{lk}, (B^{sh}_{lk})$	(shunt) susceptance of the line between bus l and bus k, in pu.
B'_{lk}	$B'_{lk} = B_{lk} - B^{sh}_{lk}$.
T'_{dj}, T'_{qj}	d- and q-axis open circuit transient time constants of jth machine, in s.
x_{d_j}, x_{q_j}	d- and q-axis synchronous reactances of jth machine, in pu.
x'_{d_j}, x'_{q_j}	d- and q-axis transient reactances of jth machine, in pu.
x''_{d_j}, x''_{q_j}	$x''_{d_j} = x_{d_j} - x'_{d_j}$, $x''_{q_j} = x_{q_j} - x'_{q_j}$.
x'_{dq_j}, p_j	$x'_{dq_j} = x'_{d_j} - x'_{q_j}$, $p_j = x_{d_j}/(T'_{dj} x'_{d_j} x''_{d_j})$.
$\lambda_{1l}, \lambda_{2l}$	Unknown bounds of $\lvert\dot{V}_{t_l}\rvert/x'_{d_l}$ and $\lvert\dot{\theta}_l\rvert/x'_{d_l}$.
c_{1j}	Positive constants to be tuned.
μ_{1j}, μ_{2j}	Positive small constants (< 1) to be tuned.
ϕ_{dj}	$\phi_{dj} = \frac{x_{q_j}}{T'_{qj} x'_{q_j}} \tilde{V}_{sj} + (\omega_j - \dot{\theta}_j) V_{q_j} + \dot{V}_{t_j} \sin \tilde{\delta}_j$.
ϕ_{qj}	$\phi_{qj} = \frac{x_{d_j}}{T'_{dj} x'_{d_j}} \tilde{V}_{cj} + (\omega_j - \dot{\theta}_j) V_{d_j} + \dot{V}_{t_j} \cos \tilde{\delta}_j$.
ψ_{pj}	$\psi_{pj} = P_{e_j}/V_{t_j}$.
ψ_{dj}	$\psi_{dj} = Q_{e_j}/V_{t_j} + V_{t_j}/x'_{d_j}$.
ψ_{qj}	$\psi_{qj} = Q_{e_j}/V_{t_j} + V_{t_j}/x'_{q_j}$.
S_{dj}	$S_{dj} = \sqrt{\psi^2_{pj} + \psi^2_{dj}}$.
S_{qj}	$S_{qj} = \sqrt{\psi^2_{pj} + \psi^2_{qj}}$.
α_{dj}	$\alpha_{dj} = \tilde{\delta}_j - \arctan(\psi_{pj}/\psi_{dj})$.
α_{qj}	$\alpha_{qj} = \tilde{\delta}_j - \arctan(\psi_{pj}/\psi_{qj})$.
φ_{1j}	$\varphi_{1j} = \cos \tilde{\delta}_j + \sin \tilde{\delta}_j \tan \alpha_{dj0}$.

Yong Wan is with the College of Automation Engineering and the Jiangsu Key Laboratory of Internet of Things and Control Technologies, Nanjing University of Aeronautics and Astronautics, Nanjing, China. E-mail: wanyong@nuaa.edu.cn, wanyong17007@163.com

Federico Milano is with the School of Electrical and Electronic Engineering, University College Dublin, Belfield, Ireland. E-mail: federico.milano@ucd.ie

Yong Wan is supported by the National Natural Science Foundation of China, under Grant No. 61403194 and Grant No. 61473145, and by the Natural Science Foundation of Jiangsu Province, under Grant No. BK20140836.

Federico Milano is supported by the Science Foundation Ireland, under Investigator Programme Grant No. SFI/15/IA/3074, and by the European Community, under EC Marie Skłodowska-Curie Career Integration Grant No. PCIG14-GA-2013-630811.

φ_{2j}	$\varphi_{2j} = \sin\tilde{\delta}_j - \cos\tilde{\delta}_j \tan\alpha_{dj0}.$
φ_{3j}	$\varphi_{3j} = V_{d_j} + V_{q_j} \tan\alpha_{dj0}.$
φ_{4j}	$\varphi_{4j} = \varphi_{1j} \tanh(\tilde{E}_{qj}\varphi_{1j}/\mu_{1j}).$
φ_{5j}	$\varphi_{5j} = V_{t_j}\varphi_{2j} \tanh(\tilde{E}_{qj}V_{t_j}\varphi_{2j}/\mu_{2j}).$
$\tilde{V}'_{sj}$	$\tilde{V}'_{sj} = \tilde{V}_{sj} \tan\alpha_{dj0}.$
Ξ_j	$\Xi_j = \frac{D_j}{\omega_s}\omega_j^2 + p_j \frac{x_{d_j}}{x'_{d_j}}\tilde{E}_{qj}^2 + \frac{x_{q_j}^2}{T'_{q_j}x'^2_{q_j}x''_{q_j}}\tilde{E}_{dj}^2.$
Ξ'_j	$\Xi'_j = \Xi_j + p_j c_{1j}\tilde{E}_{qj}^2.$
Θ_j	$\Theta_j = \mu_{1j}\lambda_{1j} + \mu_{2j}\lambda_{2j}.$

I. Introduction

HIGH-VOLTAGE transmission systems are complex, interconnected systems, whose dynamic response, stability analysis and control have been object of intense study in the last century. Due to the large number of equations and constraints that describe real-world power systems, and the resulting high complexity, most techniques aimed at defining and improving transient stability following large disturbances, are generally based on *limited simplified models* [1]–[4]. By utilizing such simplified models, a number of control technologies are presented to design effective excitation controllers [5]. In fact, in the realistic applications, the more accurate the model is, the better performance the designed control system has, but also the more challenges one needs to address [6]. RNM and SPM are two types of power system models for the excitation control problem. We will, respectively, discuss their properties and relative merits in the following part.

In the existing literature, various RNMs were presented through *eliminating the network topology and the loads* by utilizing the integral manifold method [7], [8] or the singular perturbation approach [9]–[12], or by explicitly solving the power flow constraints under the constant impedance loads assumption [13]. The RNMs are a set of *nonlinear ordinary differential equations*, so the conventional control methods *can be applied* to obtain many interesting results with the help of Lyapunov functions, for instance, adaptive backstepping, L_2 disturbance attenuation, dynamic surface, neural network and high-order sliding-mode methods have been utilized to design robust nonlinear excitation controllers [14]–[20], and a centralized excitation control law has been designed by using the Hamiltonian function method [21]. Nevertheless, RNMs only include the limited terms related to generator buses rather than the whole network buses, i.e., the load bus voltages are neglected in RNMs. Thus, as pointed out in our aforementioned discussion, the performances of the corresponding designed excitation control systems may be not satisfactory in the realistic applications.

Differing from these, the SPM was firstly proposed in [22] and it *naturally preserves the physical meanings of power network components*. But since the SPM is a set of *nonlinear differential-algebraic equations*, many classical control techniques, e.g., backstepping, *cannot be applied directly*. Only a few works investigated how to overcome the limit of the *SPM-based* transient stability assessment and control. In [23], [24], the immersion and invariance method has been applied to a differential algebraic single-machine power system to design an excitation controller. But as stated in [25], this work neglected the reactive power balance and the considered model was not correct. Besides, there are also other beneficial results with the key idea of constructing *energy functions*. For example, in [26]–[28], Lyapunov-like energy functions have been constructed to perform transient stability analysis based on the traditional swing equation dynamic model which is *a simplified SPM*; and in [29], energy-shaping technologies have been used to design decentralized excitation controller. However, the existing works *neglect the transient effects of the damper winding and the transient saliency* which are significant factors, due to the intrinsic difficulties encountered in constructing Lyapunov functions and the controller singularity problem (see Section III-B for further explanation). In addition, the fact that *the dynamic models of bus voltage magnitudes and angles and the exact values of SPM parameters*, while they also play an important role in transient stability studies, are generally unknown, and this should be considered in the excitation controller design.

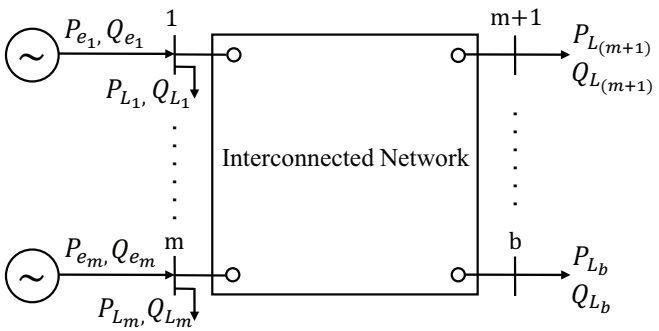

Fig. 1: An m-machine b-bus structure preserving power system with nonlinear loads.

In summary, for transient stability problem, it is necessary to comprehensively consider the aforementioned factors on the SPM, and then to tackle the corresponding challenges. Therefore, this paper proposes an extended Lyapunov-like energy function and a nonlinear adaptive decentralized excitation control strategy to improve transient stability of a structure preserving power system with nonlinear loads. Compared with the previous works, the main features of the proposed controller are threefold: (i) the design of the controller is based on relatively accurate power system model; (ii) only local machine quantities are needed to design the controller; and (iii) adaptive scheme is given to maintain robustness of excitation system even though there are unknown or varying in the SPM parameters involved by sudden and severe disturbances.

The remainder of the paper is organized as follows: Section II describes a high-order SPM. Section III proposes an extended Lyapunov-like energy function. In Section IV, a nonlinear adaptive decentralized excitation controller is designed based on the proposed energy function. The controller evaluation results are presented in Section V. Conclusions are drawn in Section VI.

II. Structure Preserving Model

We consider an m-machine b-bus structure preserving power system shown in Figure 1. Without loss of generality, the two-axis model is utilized for all m machines. The following notation is adopted in the remainder of the paper:

1. If $l \notin \bar{m}$, then $P_{e_l} = Q_{e_l} = 0$.
2. If $k \notin \Omega_l$, then $B_{lk} = B_{lk}^{sh} = 0$.

The following models are assumed for the generators, transmission lines and loads.

A. Generator Model

In this paper, we consider a fourth-order synchronous machine model [3], [4], as follows:

$$\begin{aligned} \dot{\delta}_j &= \omega_j, \\ \dot{\omega}_j &= -\tfrac{D_j}{H_j}\omega_j + \tfrac{\omega_s}{H_j}(P_{m_j} - P_{e_j}), \\ T'_{qj}\dot{E}'_{d_j} &= \tfrac{x''_{q_j}}{x'_{q_j}}V_{d_j} - \tfrac{x_{q_j}}{x'_{q_j}}E'_{d_j}, \\ T'_{dj}\dot{E}'_{q_j} &= \tfrac{x''_{d_j}}{x'_{d_j}}V_{q_j} - \tfrac{x_{d_j}}{x'_{d_j}}E'_{q_j} + E_{fd_j}, \end{aligned} \tag{1}$$

$$\begin{aligned} P_{e_j} &= \tfrac{1}{x'_{q_j}}E'_{d_j}V_{q_j} - \tfrac{1}{x'_{d_j}}E'_{q_j}V_{d_j} - \tfrac{x'_{dq_j}}{x'_{d_j}x'_{q_j}}V_{d_j}V_{q_j}, \\ Q_{e_j} &= \tfrac{1}{x'_{q_j}}E'_{d_j}V_{d_j} + \tfrac{1}{x'_{d_j}}E'_{q_j}V_{q_j} - \tfrac{1}{x'_{q_j}}V_{d_j}^2 - \tfrac{1}{x'_{d_j}}V_{q_j}^2. \end{aligned} \tag{2}$$

Note that: The excitation voltage E_{fd_j} is equivalently transformed into $E_{fd_j} = E_{fd_{j0}} + u_j$, u_j is excitation control input.

B. Lossy Network Model

The transmission lines are modeled with the standard lumped Π circuit [1]

$$\begin{aligned} P_{lk} &= G_{lk}V_{t_l}^2 + V_{t_l}V_{t_k}(B_{lk}\sin\theta_{lk} - G_{lk}\cos\theta_{lk}), \\ Q_{lk} &= B'_{lk}V_{t_l}^2 - V_{t_l}V_{t_k}(B_{lk}\cos\theta_{lk} + G_{lk}\sin\theta_{lk}). \end{aligned} \tag{3}$$

C. Load Model

The loads at each bus are represented by the following arbitrary functions of the voltage and the angle at the bus

$$P_{L_l} = f_{pl}(\theta_l), \quad Q_{L_l} = f_{ql}(V_{t_l}). \tag{4}$$

Note that, for the definition of the proposed control scheme, the expression of f_{pl} and f_{ql} do not need to be known explicitly. Finally, load power consumptions are linked to the grid through well-known power flow equations:

$$\begin{aligned} P_l &:= -P_{e_l} + P_{L_l} + \textstyle\sum_{k=1}^{b} P_{lk} = 0, \\ Q_l &:= (-Q_{e_l} + Q_{L_l} + \textstyle\sum_{k=1}^{b} Q_{lk})/V_{t_l} = 0. \end{aligned} \tag{5}$$

III. Lyapunov-like Energy Function

In this subsection, we define a *Lyapunov-like energy function* that has a unique minimum on the operating point of structure preserving power system model consisting of (1), (2), (3), (4), and (5).

A. Structure Preserving Energy Function

In [30], the nonexistence of an energy function of a lossy power system has been shown. Thus, a necessary condition for the success of the energy function method is that the network is assumed to be lossless, i.e., $G_{lk} = 0$. This is a general assumption which has been widely used in power systems analysis and control [19], [21], [27]–[29], [31], [32]. The few attempts to remove the constraint $G_{lk} = 0$, appears to be limited to small examples (see, for example, [33]). We will, hence, assume a lossless transmission system. Note, however, that this assumption does not affect the resulting control scheme, as discussed in the case study.

We consider the following energy function:

$$\begin{aligned} E(\boldsymbol{x}) = \sum_{j=1}^{m} \Big(& - P_{m_j}\delta_j + \frac{H_j}{2\omega_s}\omega_j^2 + \frac{x_{q_j}}{2x'_{q_j}x''_{q_j}}\tilde{E}_{dj}^2 \\ & + \frac{x_{d_j}}{2x'_{d_j}x''_{d_j}}\tilde{E}_{qj}^2 - \frac{E'_{dj0}}{x'_{q_j}}V_{d_j} - \frac{E'_{qj0}}{x'_{d_j}}V_{q_j} \\ & + \frac{x'_{d_j} + x'_{q_j}}{4x'_{d_j}x'_{q_j}}V_{t_j}^2 + \frac{x'_{dq_j}}{4x'_{d_j}x'_{q_j}}(V_{d_j}^2 - V_{q_j}^2)\Big) \\ & + \sum_{l=1}^{b}\sum_{k=1}^{b}\Big(B'_{lk}\int_{V_{t_{l0}}}^{V_{t_l}} x_l \mathrm{d}x_l - \frac{B_{lk}}{2}V_{t_l}V_{t_k}\cos\theta_{lk}\Big) \\ & + \sum_{l=1}^{b}\Big(\int_{V_{t_{l0}}}^{V_{t_l}} \frac{f_{ql}(x_l)}{x_l}\mathrm{d}x_l + \int_{\theta_{l0}}^{\theta_l} f_{pl}(x_l)\mathrm{d}x_l\Big). \end{aligned} \tag{6}$$

Proposition 1. The operating point $\boldsymbol{x_0}$ is the unique minimum of the energy function E in (6) based on the facts:

$$\tfrac{\partial E}{\partial \boldsymbol{x}} \mid_{\boldsymbol{x}=\boldsymbol{x_0}} = \mathbf{0}, \tag{7}$$

$$\mathrm{Hess}(E) \mid_{\boldsymbol{x}=\boldsymbol{x_0}} > 0. \tag{8}$$

Proof. See the Appendix. □

According to the proposition above, $E(\boldsymbol{x})$ is a Lyapunov-like energy function.

It is important to note that (6) is not unique. As a matter of fact, in the literature, several other energy functions have been proposed [4]. For example, the following energy function is often employed to analyze the stability of the *open-loop* power system (i.e. for $u_j = 0$):

$$\begin{aligned} E'(\boldsymbol{x}) = E(\boldsymbol{x}) + \sum_{j=1}^{m}\Big(&\frac{E'_{dj0}}{x'_{q_j}}V_{d_j} + \frac{E'_{qj0}}{x'_{d_j}}V_{q_j} \\ &+ \frac{1}{x'_{q_j}}E'_{d_j}\tilde{V}_{sj} - \frac{1}{x'_{d_j}}E'_{q_j}\tilde{V}_{cj}\Big). \end{aligned} \tag{9}$$

Proposition 2. E' in (9) satisfies the conditions:

$$\tfrac{\partial E'}{\partial \boldsymbol{x}} \mid_{\boldsymbol{x}=\boldsymbol{x_0}} = \mathbf{0}, \tag{10}$$

$$\dot{E}' \leqslant 0. \tag{11}$$

Proof. See reference [4]. □

The method proposed in [34] to justify the positive definiteness of the Hessian matrix of (9) is computationally very demanding and, for large systems, it is actually not possible to decide whether E' is a Lyapunov function. This is the main weakness of the "open-loop" analysis framework and several other energy functions considered in the literature and the main motivation for proposing (6). In the remainder of the paper, we will study the nonlinear excitation control synthesis and analyze the stability of the closed-loop power system based on the Lyapunov-like energy function E given in (6).

B. Problem Statement

Based on SPM, i.e., (1), (2), (3), (4), (5) and (19) as described in Section II and in Appendix, respectively, the time derivative of $E(\boldsymbol{x})$ along the system trajectory is

$$\dot{E} = \sum_{j=1}^{m} \Big[-\Xi_j + \frac{\tilde{E}_{qj}}{x'_{d_j}} \big(\phi_{qj} + \frac{x_{d_j}}{T'_{dj} x''_{d_j}} u_j \big) - \frac{\tilde{E}_{dj}}{x'_{q_j}} \phi_{dj} \Big]. \quad (12)$$

Through the observation of (12), the following remarks constitute relevant challenges for the design of the excitation control:

1. It is difficult to cancel the nonlinear function term $\tilde{E}_{dj}\phi_{dj}/x'_{q_j}$ through the control input u_j, because of controller singularity.
2. Due to the implicit form of V_{t_l} and θ_l, the dynamics $\dot{V}_{t_l} := f_{v_l}(t)$ and $\dot{\theta}_l := f_{\theta_l}(t)$ in eq. (5) are unknown.
3. The exact values of power system parameters are known with a certain degree of uncertainty.

These challenges are addressed in the following section.

IV. Excitation Control based on Energy Function

From Proposition 1 given in Section III-A, a natural idea to ensure post-fault transient stability is to impose that the time derivative of the energy function $E(\boldsymbol{x})$ is non-positive. This condition is direct consequence of Lyapunov second stability method. With this aim, in this section, an adaptive decentralized control scheme is proposed to solve the difficulties discussed in Section III-B.

A. Preliminaries

We first introduce the following two standard assumptions to make the control synthesis tractable.

Assumption 1. The following approximate expressions of $\tilde{E}_{qj}$ and $\tilde{E}_{dj}$ are used for the control synthesis:

$$\tilde{E}_{dj}/x'_{q_j} \doteq -\tilde{E}_{qj} \tan\alpha_{dj0}/x'_{d_j}. \quad (13)$$

Assumption 2. There exist unknown positive constants $\lambda_{1l}, \lambda_{2l}$ such that $|f_{v_l}(t)|/x'_{d_l} < \lambda_{1l}$ and $|f_{\theta_l}(t)|/x'_{d_l} < \lambda_{2l}$.

Remark 1. Note that, based on (2), and using triangle function identities, one can get the following expressions:

$$\begin{aligned} E'_{q_j}/x'_{d_j} &= S_{dj}\cos\alpha_{dj}, \\ E'_{d_j}/x'_{q_j} &= -S_{qj}\sin\alpha_{qj}. \end{aligned} \quad (14)$$

Thus, one can conclude that the values of E'_{q_j} (E'_{d_j}) depend much more on S_{dj} (S_{qj}) than on α_{dj} (α_{qj}). Moreover, since $x'_{d_j} \doteq x'_{q_j}$, then $S_{dj} \doteq S_{qj}$ and $\alpha_{dj} \doteq \alpha_{qj}$. Hence, Assumption 1 is reasonable.

Remark 2. As stated in Remark 1, Assumption 1 is a conventional hypothesis for establishing a relationship between $\tilde{E}_{qj}$ and $\tilde{E}_{dj}$ to avoid the singularity problem. In addition, based on power flow equation (5) and the implicit function theorem, the time derivatives of implicit algebraic variables (V_{t_j}, θ_j) can be deduced as nonlinear functions of system variables $\boldsymbol{x}$ which are known to be bounded (see [19]) by means of various protection schemes such as operating security limits. Therefore, the dynamics $\dot{V}_{t_l}$ and $\dot{\theta}_l$ are also bounded and Assumption 2 with unknown bounds is reasonable.

Lemma 1. The following inequality holds for any $\varepsilon > 0$ and for any $\zeta \in \mathbb{R}$

$$0 \leqslant |\zeta| - \zeta\tanh(\zeta/\varepsilon) \leqslant \kappa\varepsilon, \quad (15)$$

κ is a constant that satisfies $\kappa = e^{-(\kappa+1)}$, i.e. $\kappa = 0.2785$.

Proof. See reference [35]. □

In the following, Lemma 1 will be utilized to process the uncertainties resulting from unknown bounds λ_{1l} and λ_{2l} in the proposed adaptive control design and analysis.

B. Excitation Controller Design

AEC, for which only local information is needed, is proposed as follows.

First, let $\hat{\vartheta}_{kj}(k = 1, ..., 5)$ denote the parametric estimates and define $\tilde{\vartheta}_{1j} = \hat{\vartheta}_{1j} - \frac{x''_{d_j}}{x'_{d_j}}$, $\tilde{\vartheta}_{2j} = \hat{\vartheta}_{2j} - \frac{x_{q_j} T'_{dj} x''_{d_j}}{x_{d_j} T'_{qj} x'_{q_j}}$, $\tilde{\vartheta}_{3j} = \hat{\vartheta}_{3j} - \frac{T'_{dj} x''_{d_j}}{x_{d_j}}$, $\tilde{\vartheta}_{4j} = \hat{\vartheta}_{4j} - \frac{\lambda_{1j}}{p_j}$, $\tilde{\vartheta}_{5j} = \hat{\vartheta}_{5j} - \frac{\lambda_{2j}}{p_j}$ as the parameter estimation errors.

Then, consider the augmented Lyapunov function $W = E + \frac{p_j}{2}\sum_{k=1}^{5}\sum_{j=1}^{m}\tilde{\vartheta}_{kj}^2$. Invoking (12) and (13), we obtain:

$$\begin{aligned} \dot{W} = \sum_{j=1}^{m} \Big(& -\Xi_j + p_j\tilde{E}_{qj}u_j \\ & + p_j\big[(\hat{\vartheta}_{1j} - \tilde{\vartheta}_{1j})\tilde{E}_{qj}\tilde{V}_{cj} + \tilde{\vartheta}_{1j}\dot{\hat{\vartheta}}_{1j}\big] \\ & + p_j\big[(\hat{\vartheta}_{2j} - \tilde{\vartheta}_{2j})\tilde{E}_{qj}\tilde{V}'_{sj} + \tilde{\vartheta}_{2j}\dot{\hat{\vartheta}}_{2j}\big] \\ & + p_j\big[(\hat{\vartheta}_{3j} - \tilde{\vartheta}_{3j})\tilde{E}_{qj}\omega_j\varphi_{3j} + \tilde{\vartheta}_{3j}\dot{\hat{\vartheta}}_{3j}\big] \\ & + p_j\big[(\hat{\vartheta}_{4j} - \tilde{\vartheta}_{4j})\tilde{E}_{qj}\varphi_{4j} + \tilde{\vartheta}_{4j}\dot{\hat{\vartheta}}_{4j}\big] \\ & + p_j\big[(\hat{\vartheta}_{5j} - \tilde{\vartheta}_{5j})\tilde{E}_{qj}\varphi_{5j} + \tilde{\vartheta}_{5j}\dot{\hat{\vartheta}}_{5j}\big] \\ & + \big(\frac{\dot{V}_{t_j}}{x'_{d_j}}\tilde{E}_{qj}\varphi_{1j} - \lambda_{1j}\tilde{E}_{qj}\varphi_{4j}\big) \\ & + \big(\frac{\dot{\theta}_j}{x'_{d_j}}\tilde{E}_{qj}V_{t_j}\varphi_{2j} - \lambda_{2j}\tilde{E}_{qj}\varphi_{5j}\big)\Big). \end{aligned} \quad (16)$$

Finally, the control signal u_j, which incorporates adaptive updating laws of unknown parameters, is designed as follows:

$$\begin{aligned} &\dot{\hat{\vartheta}}_{1j} = \tilde{E}_{qj}\tilde{V}_{cj}, \dot{\hat{\vartheta}}_{2j} = \tilde{E}_{qj}\tilde{V}'_{sj}, \dot{\hat{\vartheta}}_{3j} = \tilde{E}_{qj}\omega_j\varphi_{3j}, \\ &\dot{\hat{\vartheta}}_{4j} = \tilde{E}_{qj}\varphi_{4j}, \dot{\hat{\vartheta}}_{5j} = \tilde{E}_{qj}\varphi_{5j}, \\ &\phi_j = \hat{\vartheta}_{1j}\tilde{V}_{cj} + \hat{\vartheta}_{2j}\tilde{V}'_{sj} + \hat{\vartheta}_{3j}\omega_j\varphi_{3j}, \\ &\chi_j = \hat{\vartheta}_{4j}\varphi_{4j} + \hat{\vartheta}_{5j}\varphi_{5j}, \\ &u_j = -(\phi_j + \chi_j + c_{1j}\tilde{E}_{qj}). \end{aligned} \quad (17)$$

In order to clearly show the above controller, block diagram is given in Figure 2. Substituting (17) into (16) and applying Lemma 1, we obtain:

$$\begin{aligned} \dot{W} &< \sum_{j=1}^{m}\big[-\Xi'_j + \lambda_{1j}\big(|\tilde{E}_{qj}\varphi_{1j}| - \tilde{E}_{qj}\varphi_{4j}\big) \\ &\qquad + \lambda_{2j}\big(|\tilde{E}_{qj}V_{t_j}\varphi_{2j}| - \tilde{E}_{qj}\varphi_{5j}\big)\big] \\ &\leqslant \sum_{j=1}^{m}(-\Xi'_j + \kappa\Theta_j). \end{aligned} \quad (18)$$

The inequality (18) indicates that the proposed control scheme is stable in the Lyapunov sense.

Remark 3. In the post-fault transient, system trajectories can deviate from their equilibrium points and lead the term

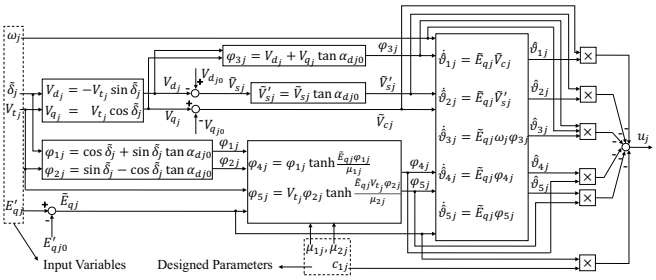

Fig. 2: Block diagram of AEC model (17).

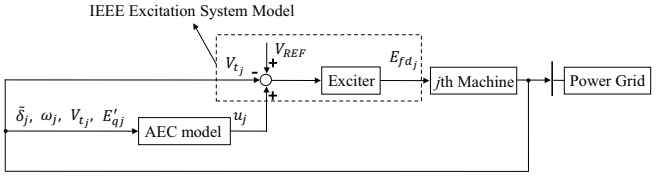

Fig. 3: Schematic view of implementation of AEC model (17).

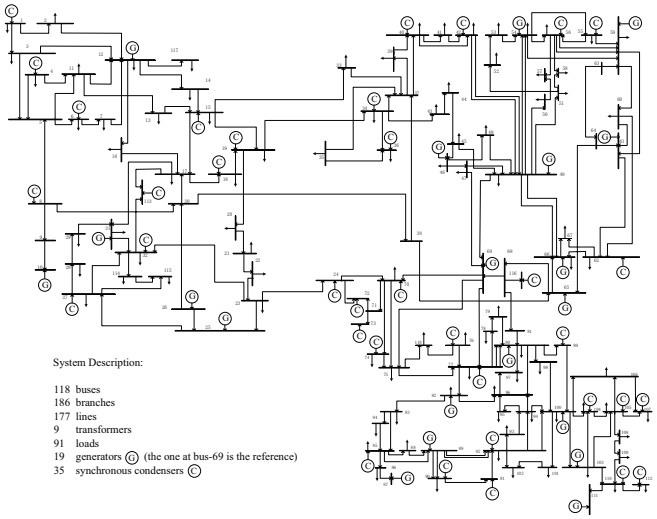

Fig. 4: IEEE 118-bus system.

$\sum_{j=1}^{m} \Xi'_j$ to be large compared with $\kappa \sum_{j=1}^{m} \Theta_j$. Therefore, the designed AEC as shown in (17) provides decreasing of Lyapunov function W along the post-fault system trajectory such that the power system will asymptotically converge to the region $\|\boldsymbol{x} - \boldsymbol{x_0}\| \leqslant \sqrt{\kappa \sum_{j=1}^{m} \Theta_j}$ with arbitrarily small constants μ_{1j} and μ_{2j}.

Remark 4. For practical implementation of the proposed adaptive excitation system model, a conventional approach as shown in Figure 3 (see [36] for reference) is to add the AEC output signal u_j to the voltage reference set point (V_{REF}, see [37] for details) to produce an error voltage for the exciter which is equipped on jth generator. In other words, the proposed AEC is actually implemented as an additional signal added to the voltage error calculation, i.e., automatic voltage regulator (AVR) summing input [37]. In steady state, this signal u_j is zero. As such, the main structure of the existing excitation system (AVR) is not altered.

Remark 5. There are three parameters c_{1j}, μ_{1j} and μ_{2j} to be tuned for the AEC of jth generator. First, choose any initial values $0 < c_{1j}^0$, $0 < \mu_{1j}^0 < 1$ and $0 < \mu_{2j}^0 < 1$. Then, under large disturbance test mode, if large overshoot of voltage happens, set $c_{1j} = c_{1j}^1 > c_{1j}^0$, $\mu_{1j} = \mu_{1j}^1 > \mu_{1j}^0$ and $\mu_{2j} = \mu_{2j}^1 > \mu_{2j}^0$. However, larger values of designed parameters may cause larger oscillation of relative speed, thus a trade-off between voltage and relative speed may have to be made heuristically.

V. Controller Performance Evaluation

The IEEE 118-bus 54-unit interconnected power system shown in Figure 4 is utilized to evaluate the performance of the proposed AEC. The on-line capacity is $P = 9966$ MW, $Q = -7345 \sim 11777$ MVAr. The total load is $P_L = 4242$ MW, $Q_L = 1438$ MVAr. Due to space limitation, system data (such as power flow solution, generator parameters, line conductance and susceptance, etc.) is omitted but the interested reader can find more details in [1].

All simulations are carried out using MatDyn [38] and MatPower [39]. It is important to note that, although the AEC model is proposed based on the energy function with a conventional lossless approximation as described in Section III-A, the simulations are performed using the lossy network model as shown in Section II-B.

The following mean errors are defined as the simulation outputs to achieve a holistic evaluation.

$$S_\omega^n = \tfrac{1}{54}\sum_{j=1}^{54} |S_{\omega_j}|, V_t^n = \tfrac{1}{118}\sum_{l=1}^{118} |V_{t_l} - V_{t_{l0}}|,$$
$$Q_e^n = \tfrac{1}{54}\sum_{j=1}^{54} |Q_{e_j} - Q_{e_{j0}}|, E_{fd}^n = \tfrac{1}{54}\sum_{j=1}^{54} |E_{fd_j} - E_{fd_{j0}}|.$$

The performance evaluation of the designed AEC is achieved by comparing with the RNC in [18] and the standard IEEE Type DC1C/AC4C excitation systems [37]. Moreover, throughout the simulation, all 54 machines are assumed to be driven by turbines with constant mechanical output power and are represented by the fourth order model that includes the transient effects of damper winding and transient saliency.

There are three points to be explained: (i) the AEC requires the measurable relative angle ($\tilde{\delta}_j$), not each quantity (δ_j or θ_j) independently; (ii) (extended) Kalman-filter based dynamic estimators [40], [41] can be employed to estimate the q-axis stator transient voltage (E'_{q_j}) which cannot be measured directly; and (iii) the AEC does not need prior knowledge of exact values of power system parameters.

TABLE I: Comparison Scheme

Generator ES	Condenser ES	S1	S2	S3
AEC	AEC	TLO	TPSC	MF
RNC	RNC			
AC4C	DC1C			

[1] ES, TLO, TPSC, and MF mean Excitation System, Transmission Line Outage, Three-Phase Short-Circuit, and Multiple Faults.

The simulation output variables are chosen as relative rotor speed (S_{ω_j}), bus voltage magnitude (V_{t_l}), machine reactive power (Q_{e_j}), excitation voltage (E_{fd_j}) and their mean errors (S_ω^n, V_t^n, Q_e^n, E_{fd}^n) defined above, for all 54 machines ($\forall j \in \bar{m}$) and 118 buses ($\forall l \in \bar{b}$). In addition, Table I provides the simulation comparison scheme which is implemented through the following 3 scenarios (S1, S2, S3).

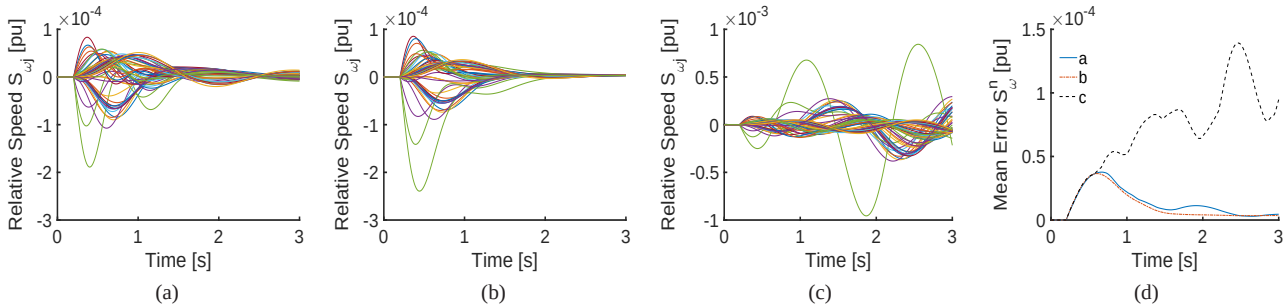

Fig. 5: Scenario 1: Relative speeds of 54 synchronous machines. (a) Proposed AEC; (b) RNC; (c) Standard IEEE controllers; (d) Comparison of mean error S^n_ω.

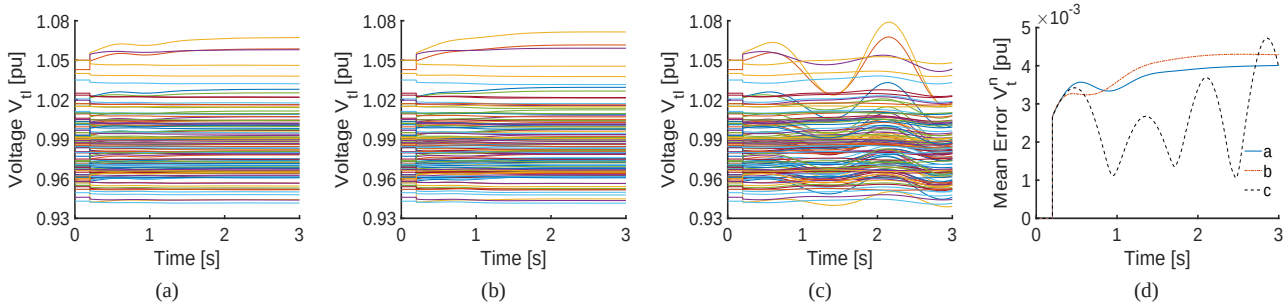

Fig. 6: Scenario 1: Voltage magnitudes of 118 Buses. (a) Proposed AEC; (b) RNC; (c) Standard IEEE controllers; (d) Comparison of mean error V^n_t.

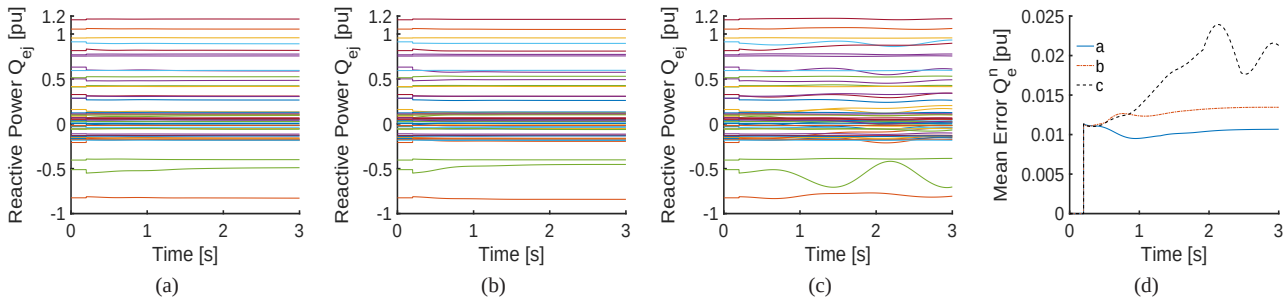

Fig. 7: Scenario 1: Reactive powers of 54 synchronous machines. (a) Proposed AEC; (b) RNC; (c) Standard IEEE controllers; (d) Comparison of mean error Q^n_e.

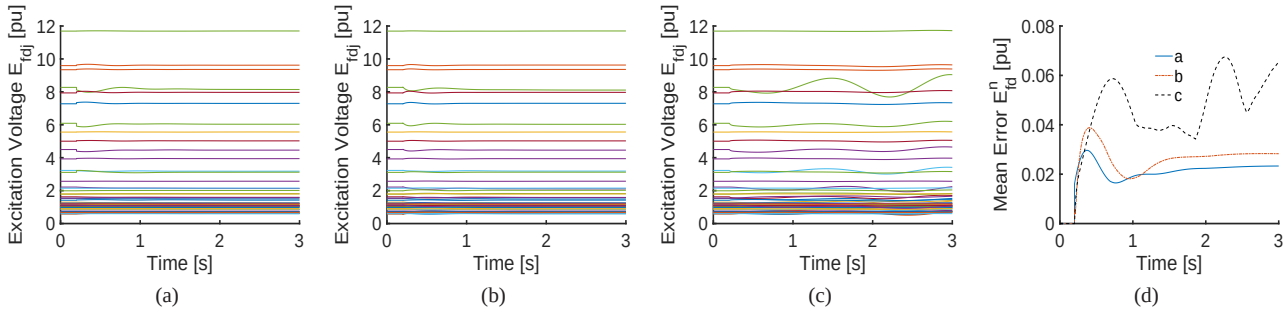

Fig. 8: Scenario 1: Excitation voltages of 54 synchronous machines. (a) Proposed AEC; (b) RNC; (c) Standard IEEE controllers; (d) Comparison of mean error E^n_{fd}.

1) Scenario 1. Transmission line outage fault: A small-disturbance test, in which outage occurs on branch between buses 30 and 38 at 0.2 s, is performed to simulate a transient reduction of the power transfer capability that can lead to power oscillations.

From figs. 5 to 8 which are the response trajectories of all output variables in this case, we find that all the three excitation models are effective to recover stable steady-state condition but, compared comprehensively (see Table II for the comparison results with 3 indexes): (i) AEC has the best voltage regulation performance with the highest accuracy and the lowest cost of control; and (ii) for the rotor speed, AEC and RNC yield similar performances which are better than those of standard IEEE controllers.

Thus, a small fault case depicted above verifies the effectiveness and the superiority of our AEC, but since there exists possibility of more serious faults in practice and it is necessary to further evaluate and compare the regulation performance of

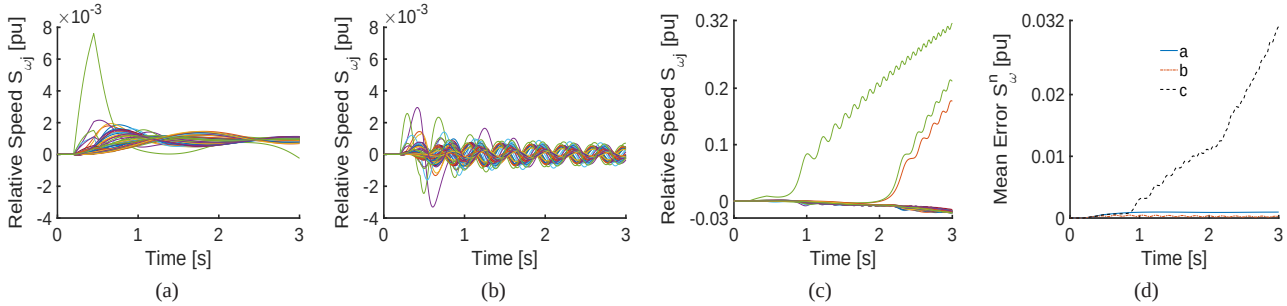

Fig. 9: Scenario 2: Relative speeds of 54 synchronous machines. (a) Proposed AEC; (b) RNC; (c) Standard IEEE controllers; (d) Comparison of mean error S^n_ω.

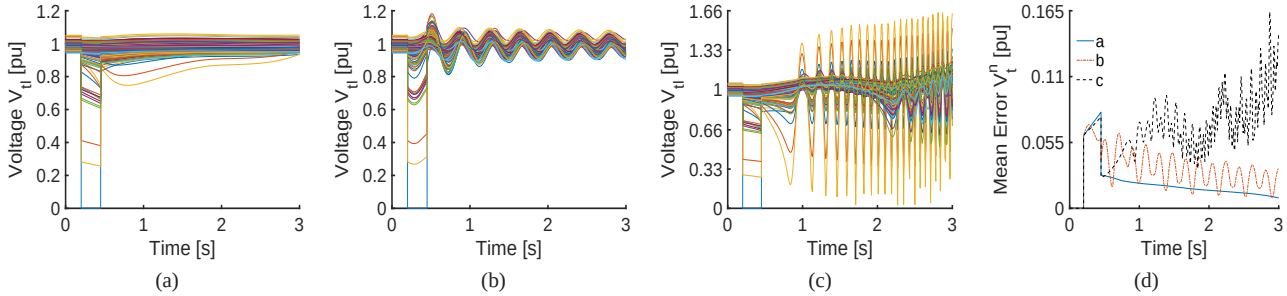

Fig. 10: Scenario 2: Voltage magnitudes of 118 Buses. (a) Proposed AEC; (b) RNC; (c) Standard IEEE controllers; (d) Comparison of mean error V^n_t.

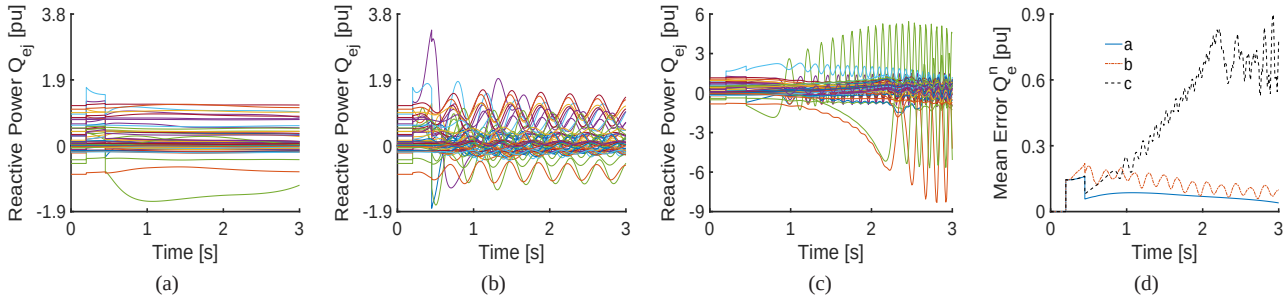

Fig. 11: Scenario 2: Reactive powers of 54 synchronous machines. (a) Proposed AEC; (b) RNC; (c) Standard IEEE controllers; (d) Comparison of mean error Q^n_e.

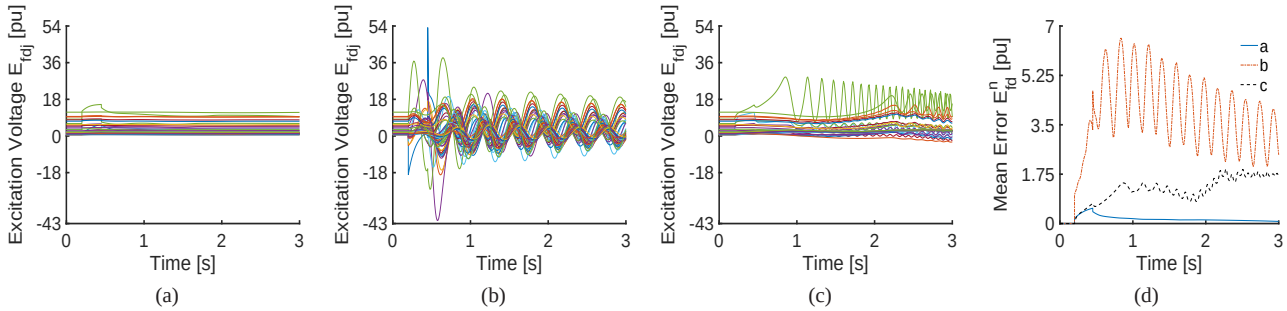

Fig. 12: Scenario 2: Excitation voltages of 54 synchronous machines. (a) Proposed AEC; (b) RNC; (c) Standard IEEE controllers; (d) Comparison of mean error E^n_{fd}.

AEC, we consider a three-phase fault in the next scenario.

2) Scenario 2. Three-phase short-circuit fault: A large disturbance namely three-phase fault that occurs on bus 1 at 0.2 s and then is cleared after 250 ms, is utilized to further evaluate our AEC. During the fault, the synchronous machine at the faulted bus cannot generate active and reactive power normally, and the voltage at this short-circuit bus will drop to zero. As such, in the post-fault period, if there is no valid excitation control, the fault may trigger critical oscillations and may eventually lead to the whole system instability.

As shown in figs. 9 to 12, the response curves of the outputs of AEC, RNC, and IEEE standard controllers, which are obtained by considering this large fault, are compared (see Table II for further results). Following this: (i) the proposed AEC is able to get the smoothest and the most stable responses and to regulate the voltages to their desired values in the most accurate way by the lowest costs of reactive power injection and field voltage control; (ii) the RNC exhibits smaller overshoot and steady-state error on the rotor speed

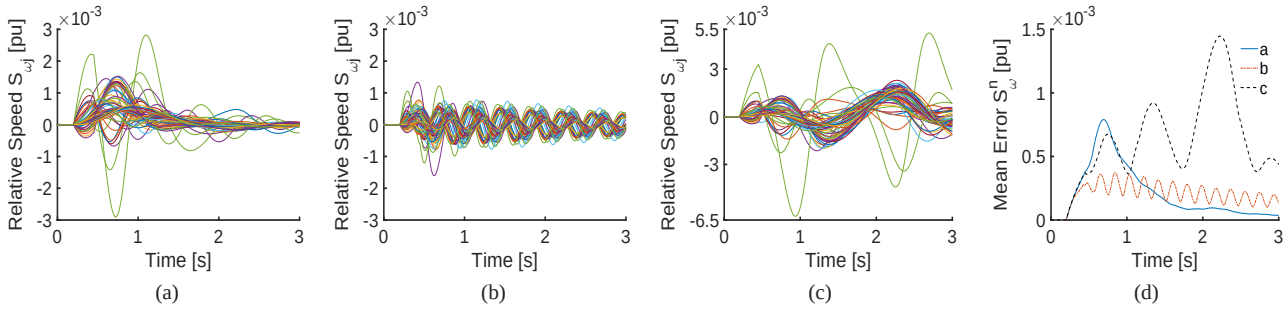

Fig. 13: Scenario 3: Relative speeds of 54 synchronous machines. (a) Proposed AEC; (b) RNC; (c) Standard IEEE controllers; (d) Comparison of mean error S^n_ω.

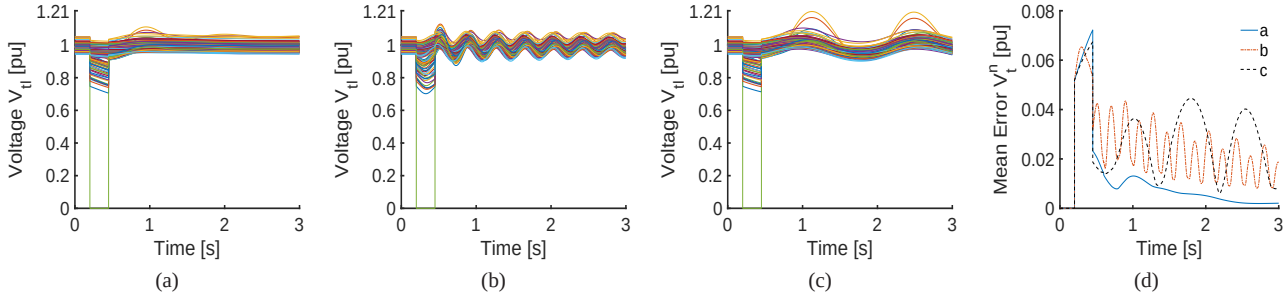

Fig. 14: Scenario 3: Voltage magnitudes of 118 Buses. (a) Proposed AEC; (b) RNC; (c) Standard IEEE controllers; (d) Comparison of mean error V^n_t.

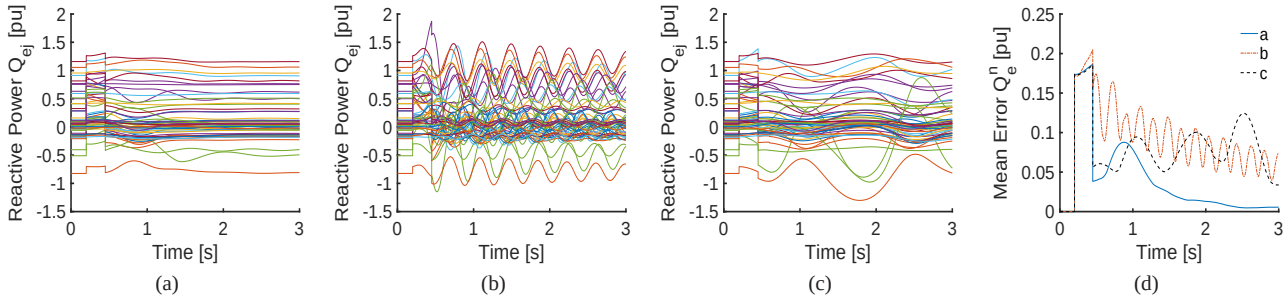

Fig. 15: Scenario 3: Reactive powers of 54 synchronous machines. (a) Proposed AEC; (b) RNC; (c) Standard IEEE controllers; (d) Comparison of mean error Q^n_e.

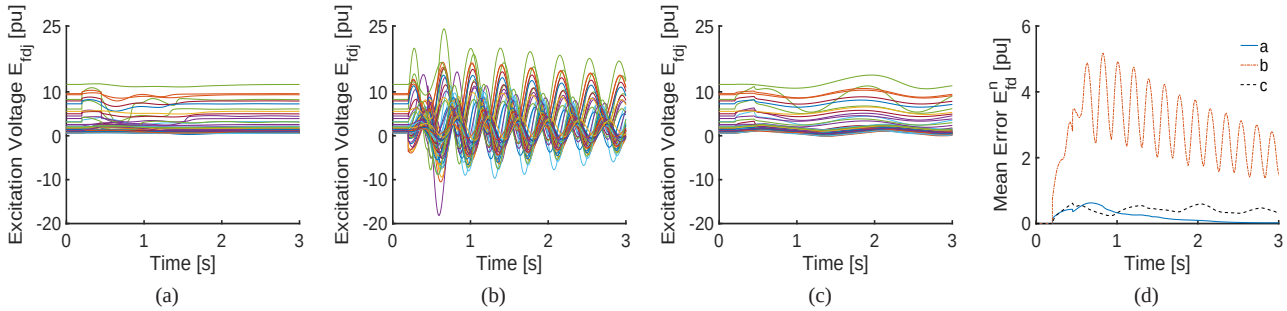

Fig. 16: Scenario 3: Excitation voltages of 54 synchronous machines. (a) Proposed AEC; (b) RNC; (c) Standard IEEE controllers; (d) Comparison of mean error E^n_{fd}.

responses of only a few machines than the AEC, but the RNC cannot eliminate high-frequency oscillation and over-voltage; and (iii) the system controlled by IEEE AC4C/DC1C, instead, is unstable.

Consequently, in comparison with RNC and IEEE controllers, the proposed AEC displays its ability to mitigate the large fault effects and to recover system steady-state in a short time. In addition, only a single fault is included in each of the above scenarios, in order to assess the performance of the AEC under a relatively complex situation, multiple faults are utilized in the next scenario.

3) Scenario 3. Multiple faults: In this case, we consider multiple faults on bus 33. At 0.2 s, three-phase short-circuit happens, after that, it is cleared at 0.45 s, and in the meanwhile, load shedding occurs. Besides the influences of three-phase fault discussed in the last scenario, the imbalance between load demand and generation may result in *frequency deviation*.

In figs. 13 to 16, we find that all the three excitation models can ensure the stability under this multiple faults

TABLE II: COMPARISON RESULTS

Best \ Output / Index		S_{ω_j}	V_{t_j}	Q_{e_j}	E_{fd_j}
OS	S1	*	RNC	AEC	AEC
	S2	*	AEC	AEC	AEC
	S3	RNC	AEC	AEC	AEC
OF	S1	RNC	*	*	*
	S2	AEC	AEC	AEC	AEC
	S3	AEC	AEC	AEC	AEC
SSE	S1	RNC	AEC	AEC	AEC
	S2	RNC	AEC	AEC	AEC
	S3	AEC	AEC	AEC	AEC

[1] OS, OF and SSE mean Overshoot, Oscillation Frequency and Steady-State Error respectively.
[2] * represents both AEC and RNC.

condition, furthermore, as depicted in Table II: (i) for both the transient process and the steady-state, the AEC exhibits the most excellent post-fault voltage regulation by spending least costs for reactive power and excitation voltage; and (ii) for the transient process, although AEC has slightly bigger amplitude of the rotor speed responses than RNC, all the output trajectories of AEC are more stable than those of RNC and IEEE controllers.

To sum up the above three scenarios, the AEC has adaptability to different fault conditions and has an outstanding regulation performance beyond conventional excitation models. This is mainly due to the fact that our AEC is derived based on the relatively accurate SPM and the proposed extended energy function which possesses both Lyapunov characteristic and physical interpretation. Additionally, the comparison results also confirm the theoretical ones given in the previous section.

VI. CONCLUSION

The paper proposes a nonlinear adaptive excitation controller that improves the dynamic response of multi-machine power systems. The main features of the proposed controller are: (i) it accounts for high-order structure preserving power system models with nonlinear loads; (ii) it requires only local measurements and data without prior knowledge of exact SPM parameters; (iii) it uses only four available variables for feedback (as discussed in Section V); and (iv) it includes only three parameters to be tuned. The results obtained in the case study show that the proposed controller outperform conventional control schemes and is able to keep the system stable also in case of large critical disturbances. Future work will focus on the analysis of the dynamic response of the proposed controller for systems with high penetration of renewables and non-synchronous generation.

APPENDIX
PROOF OF PROPOSITION 1

Proof. Differentiating E leads to:

$$\frac{\partial E}{\partial \delta_j} = P_{e_j} - P_{m_j} + \frac{1}{x'_{d_j}}\tilde{E}_{qj}V_{d_j} - \frac{1}{x'_{q_j}}\tilde{E}_{dj}V_{q_j},$$
$$\frac{\partial E}{\partial \omega_j} = \frac{H_j}{\omega_s}\omega_j,\ \frac{\partial E}{\partial E'_{q_j}} = \frac{x_{d_j}}{x'_{d_j}x''_{d_j}}\tilde{E}_{qj},\ \frac{\partial E}{\partial E'_{d_j}} = \frac{x_{q_j}}{x'_{q_j}x''_{q_j}}\tilde{E}_{dj},$$
$$\frac{\partial E}{\partial V_{t_l}} = \begin{cases} Q'_l(\delta_l, \boldsymbol{V}, \boldsymbol{\theta}), & l \in \bar{m}, \\ Q_l(\boldsymbol{V}, \boldsymbol{\theta}), & l \notin \bar{m}, \end{cases} \tag{19}$$
$$\frac{\partial E}{\partial \theta_l} = \begin{cases} P'_l(\delta_l, \boldsymbol{V}, \boldsymbol{\theta}), & l \in \bar{m}, \\ P_l(\boldsymbol{V}, \boldsymbol{\theta}), & l \notin \bar{m}, \end{cases}$$

where $P'_l = P_l + \tilde{E}_{dl}V_{q_l}/x'_{q_l} - \tilde{E}_{ql}V_{d_l}/x'_{d_l}$, $Q'_l = Q_l + \tilde{E}_{dl}V_{d_l}/(x'_{q_l}V_{t_l}) + \tilde{E}_{ql}V_{q_l}/(x'_{d_l}V_{t_l})$. The expressions shown in (19) lead to (7).

The Hessian matrix of E, calculated at the operating point, is as follows:

$$\mathrm{Hess}(E)|_{\boldsymbol{x}=\boldsymbol{x_0}} = \left[\begin{array}{c|c|cc} \frac{\partial \boldsymbol{P_e}}{\partial \boldsymbol{\delta}} & & \frac{\partial \boldsymbol{P_e}}{\partial \boldsymbol{V}} & \frac{\partial \boldsymbol{P_e}}{\partial \boldsymbol{\theta}} \\ \hline & \boldsymbol{H_x} & & \\ \hline \frac{\partial \boldsymbol{Q_f}}{\partial \boldsymbol{\delta}} & & \frac{\partial \boldsymbol{Q_f}}{\partial \boldsymbol{V}} & \frac{\partial \boldsymbol{Q_f}}{\partial \boldsymbol{\theta}} \\ \frac{\partial \boldsymbol{P_f}}{\partial \boldsymbol{\delta}} & & \frac{\partial \boldsymbol{P_f}}{\partial \boldsymbol{V}} & \frac{\partial \boldsymbol{P_f}}{\partial \boldsymbol{\theta}} \end{array}\right]\Bigg|_{\boldsymbol{x}=\boldsymbol{x_0}},$$

where $\boldsymbol{P_f} = \mathrm{col}(P_l)$, $\boldsymbol{Q_f} = \mathrm{col}(Q_l)$, $\boldsymbol{H_x} = \mathrm{diag}\big(\mathrm{diag}\{\frac{H_j}{\omega_s}\}, \mathrm{diag}\{\frac{x_{d_j}}{x'_{d_j}x''_{d_j}}\}, \mathrm{diag}\{\frac{x_{q_j}}{x'_{q_j}x''_{q_j}}\}\big)$.

From positive definite Jacobian of normal power flow which corresponds to local regularity [27], Lemma 1 in [29] and Proposition 2 in [31], one can prove (8). Since both conditions (7) and (8) are satisfied, the energy function E is Lyapunov-like function. □

REFERENCES

[1] P. M. Anderson and A. A. Fouad, *Power system control and stability, second edition*. Wiley-IEEE Press, 2002.
[2] L. L. Grigsby, *Power system stability and control, third edition*. Boca Raton: CRC Press, Taylor & Francis, 2012.
[3] K. R. Padiyar, *Power system dynamics: stability and control, second edition*. Hyderabad: BS publications, 2008.
[4] ——, *Structure preserving energy functions in power systems: theory and applications*. CRC Press, 2013.
[5] M. Ilíc, E. Allen, J. J. Chapman, C. A. King, J. H. Lang, and E. Litvinov, "Preventing future blackouts by means of enhanced electric power systems control: From complexity to order," *Proceedings of the IEEE*, vol. 93, no. 11, pp. 1920–1941, 2005.
[6] Z. Wang, L. Liu, and H. Zhang, "Neural network-based model-free adaptive fault-tolerant control for discrete-time nonlinear systems with sensor fault," *IEEE Transactions on Systems, Man, and Cybernetics: Systems*, 2017.
[7] P. W. Sauer, S. Ahmed-Zaid, and P. V. Kokotovic, "An integral manifold approach to reduced order dynamic modeling of synchronous machines," *IEEE Transactions on Power Systems*, vol. PS-3, no. 1, pp. 17–23, 1988.
[8] P. V. Kokotovic and P. W. Sauer, "Integral manifold as a tool for reduced-order modeling of nonlinear systems: A synchronous machine case study," *IEEE Transactions on Circuits and Systems*, vol. 36, no. 3, pp. 403–410, 1989.
[9] B. W. Gordon and S. Liu, "A singular perturbation approach for modeling differential-algebraic systems," *Journal of dynamic systems, measurement, and control*, vol. 120, no. 4, pp. 541–545, 1998.
[10] B. W. Gordon, "State space modeling of differential-algebraic systems using singularly perturbed sliding manifolds," Ph.D. dissertation, Massachusetts Institute of Technology, 1999.
[11] I. Martínez, A. R. Messina, and V. Vittal, "Normal form analysis of complex system models: a structure-preserving approach," *IEEE Transactions on Power Systems*, vol. 22, no. 4, pp. 1908–1915, 2007.

[12] C.-C. Chu and H.-D. Chiang, "Constructing analytical energy functions for network-preserving power system models," *Circuits, Systems and Signal Processing*, vol. 24, no. 4, pp. 363–383, 2005.

[13] W. Dib, A. E. Barabanov, R. Ortega, and F. Lamnabhi-Lagarrigue, "An explicit solution of the power balance equations of structure preserving power system models," *IEEE Transactions on Power Systems*, vol. 24, no. 2, pp. 759–765, 2009.

[14] R. Yan, Z. Y. Dong, T. K. Saha, and R. Majumder, "A power system nonlinear adaptive decentralized controller design," *Automatica*, vol. 46, no. 2, pp. 330–336, 2010.

[15] T. K. Roy, M. A. Mahmud, W. Shen, A. M. T. Oo, and M. E. Haque, "Robust nonlinear adaptive backstepping excitation controller design for rejecting external disturbances in multimachine power systems," *International Journal of Electrical Power & Energy Systems*, vol. 84, pp. 76–86, 2017.

[16] Y. Wan and B. Jiang, "Practical nonlinear excitation control for a single-machine infinite-bus power system based on a detailed model," *Automatica*, vol. 62, pp. 18–25, 2015.

[17] Y. Wang, D. Cheng, C. Li, and Y. Ge, "Dissipative Hamiltonian realization and energy-based L_2-disturbance attenuation control of multimachine power systems," *IEEE Transactions on Automatic Control*, vol. 48, no. 8, pp. 1428–1433, 2003.

[18] H. Liu, Z. Hu, and Y. Song, "Lyapunov-based decentralized excitation control for global asymptotic stability and voltage regulation of multimachine power systems," *IEEE Transactions on Power Systems*, vol. 27, no. 4, pp. 2262–2270, 2012.

[19] S. Mehraeen, S. Jagannathan, and M. L. Crow, "Power system stabilization using adaptive neural network-based dynamic surface control," *IEEE Transactions on Power Systems*, vol. 26, no. 2, pp. 669–680, 2011.

[20] H. Huerta, A. G. Loukianov, and J. M. Cañedo, "Robust multimachine power systems control via high order sliding modes," *Electric Power Systems Research*, vol. 81, no. 7, pp. 1602–1609, 2011.

[21] W. Dib, R. Ortega, A. Barabanov, and F. Lamnabhi-Lagarrigue, "A globally convergent controller for multi-machine power systems using structure-preserving models," *IEEE Transactions on Automatic Control*, vol. 54, no. 9, pp. 2179–2185, 2009.

[22] A. R. Bergen and D. J. Hill, "A structure preserving model for power system stability analysis," *IEEE Transactions on Power Apparatus and Systems*, vol. PAS-100, no. 1, pp. 25–35, 1981.

[23] N. S. Manjarekar, R. N. Banavar, and R. Ortega, "An application of immersion and invariance to a differential algebraic system: A power system," in *Control Conference (ECC), 2009 European*, 2009.

[24] ——, "An immersion and invariance algorithm for a differential algebraic system," *European Journal of Control*, vol. 18, no. 2, pp. 145–157, 2012.

[25] J. A. Acosta, "Discussion on: An immersion and invariance algorithm for a differential algebraic system," *European Journal of Control*, vol. 18, no. 2, pp. 159–161, 2012.

[26] D. J. Hill and C. N. Chong, "Lyapunov functions of luré-postnikov form for structure preserving models of power systems," *Automatica*, vol. 25, no. 3, pp. 453–460, 1989.

[27] R. J. Davy and I. A. Hiskens, "Lyapunov functions for multimachine power systems with dynamic loads," *IEEE Transactions on Circuits and Systems I: Fundamental Theory and Applications*, vol. 44, no. 9, pp. 796–812, 1997.

[28] T. L. Vu and K. Turitsyn, "Lyapunov functions family approach to transient stability assessment," *IEEE Transactions on Power Systems*, vol. 31, no. 2, pp. 1269–1277, 2016.

[29] B. He, X. Zhang, and X. Zhao, "Transient stabilization of structure preserving power systems with excitation control via energy-shaping," *International Journal of Electrical Power & Energy Systems*, vol. 29, no. 10, pp. 822–830, 2007.

[30] N. Narasimhamurthi, "On the existence of energy function for power systems with transmission losses," *IEEE Transactions on Circuits & Systems*, vol. 31, no. 2, pp. 199–203, 1984.

[31] I. A. Hiskens and D. J. Hill, "Energy functions, transient stability and voltage behaviour in power systems with nonlinear loads," *IEEE Transactions on Power Systems*, vol. 4, no. 4, pp. 1525–1533, 1989.

[32] K. L. Praprost and K. A. Loparo, "An energy function method for determining voltage collapse during a power system transient," *IEEE Transactions on Circuits and Systems I: Fundamental Theory and Applications*, vol. 41, no. 10, pp. 635–651, 1994.

[33] M. Anghel, F. Milano, and A. Papachristodoulou, "Algorithmic construction of Lyapunov functions for power system stability analysis," *IEEE Transactions on Circuits and Systems-I: Regular Papers*, vol. 60, no. 9, pp. 2533–2546, 2013.

[34] T. Yin and J. Wang, "The positive definiteness judgment of hessian matrix and its application in hamilton realization of multimachine power system," *IEEJ Transactions on Electrical and Electronic Engineering*, vol. 8, no. S1, pp. S47–S52, 2013.

[35] M. M. Polycarpou and P. A. Ioannou, "A robust adaptive nonlinear control design," *Automatica*, vol. 32, no. 3, pp. 423–427, 1996.

[36] A. Karimi, S. Eftekharnejad, and A. Feliachi, "Reinforcement learning based backstepping control of power system oscillations," *Electric Power Systems Research*, vol. 79, no. 11, pp. 1511–1520, 2009.

[37] *IEEE recommended practice for excitation system models for power system stability studies*, IEEE Power and Energy Society IEEE Std. 421.5-2016, 26 Aug. 2016.

[38] S. Cole and R. Belmans, "Matdyn, a new matlab-based toolbox for power system dynamic simulation," *IEEE Transactions on Power Systems*, vol. 26, no. 3, pp. 1129–1136, 2011.

[39] R. D. Zimmerman, C. E. Murillo-Sánchez, and R. J. Thomas, "Matpower: Steady-state operations, planning, and analysis tools for power systems research and education," *IEEE Transactions on Power Systems*, vol. 26, no. 1, pp. 12–19, 2011.

[40] A. S. Debs and R. E. Larson, "A dynamic estimator for tracking the state of a power system," *IEEE Transactions on Power Apparatus and Systems*, no. 7, pp. 1670–1678, 1970.

[41] E. Ghahremani and I. Kamwa, "Dynamic state estimation in power system by applying the extended kalman filter with unknown inputs to phasor measurements," *IEEE Transactions on Power Systems*, vol. 26, no. 4, pp. 2556–2566, 2011.

Yong Wan was born in Liaoning, China, in 1985. He received the B.E. degree from Nanjing Normal University, China, in 2008, and the M.E. and Ph.D. degrees from Northeastern University, China, in 2010 and 2013 respectively, all in Automatic Control. In 2014, he joined College of Automation Engineering in Nanjing University of Aeronautics and Astronautics, China, where he is currently a lecturer. His research interests include power system control and stability, nonlinear adaptive control.

Federico Milano (S'02, M'04, SM'09, F'16) received from the Univ. of Genoa, Italy, the ME and Ph.D. in Electrical Eng. in 1999 and 2003, respectively. From 2001 to 2002 he was with the Univ. of Waterloo, Canada, as a Visiting Scholar. From 2003 to 2013, he was with the Univ. of Castilla-La Mancha, Spain. In 2013, he joined the Univ. College Dublin, Ireland, where he is currently Professor of Power Systems Control and Protections. His research interests include power system modelling, control and stability analysis.